Elevating Endogenous Sphingosine-1-Phosphate (S1P) Levels Improves Endothelial Function and Ameliorates Atherosclerosis in Low Density Lipoprotein Receptor-Deficient (LDL-R-/-) Mice

ELEVATING ENDOGENOUS SPHINGOSINE 1-PHOSPHATE (S1P) LEVELS IMPROVES ENDOTHELIAL FUNCTION AND AMELIORATES ATHEROSCLEROSIS IN LOW DENSITY LIPOPROTEIN RECEPTOR-DEFICIENT (LDL-R$^{-/-}$) MICE[1]

Renata Feuerborn[1*], Manuela Besser[2*], Francesco Potì[3,4],

Ralph Burkhardt[5], Gabriele Weißen-Plenz[1], Uta Ceglarek[5], Manuela Simoni[4]

Richard L. Proia[6], Hendrik Freise[2], and Jerzy-Roch Nofer[1]

1. Center for Laboratory Medicine, University Hospital Münster, Münster, Germany 2. Department of Anaesthesiology and Intensive Medicine, University Hospital Münster, Münster, Germany 3. Department of Medicine and Surgery – Unit of Neurosciences, University of Parma, Parma, Italy 4. Unit of Endocrinology, Department of Biomedical, Metabolic and Neural Sciences, University of Modena and Reggio Emilia, Italy 5. Institute of Laboratory Medicine, Clinical Chemistry and Molecular Diagnostics, University Hospital Leipzig, Leipzig, Germany 6. Genetics of Development and Disease Branch, National Institute of Diabetes and Digestive and Kidney Diseases, National Institutes of Health, Bethesda, MD, USA

Short running title: Nofer et al.: S1P, endothelial cells and atherosclerosis

Total word count: 4321 (excluding figure legends and references)

Abstract word count: 246

Number of references: 46

* equal contribution

Address correspondence to:

Jerzy-Roch Nofer, M.D., M.B.A.
Centrum für Laboratoriumsmedizin
Universitätsklinikum Münster
Albert Schweizer Campus 1, Gebäude A1
48149 Münster, Germany.
TL: +492518347228
Fax: +492518347225
e-mail: nofer@uni-muenster.de

[1] Financial support: Grant NO406/3-1 from Deutsche Forschungsgemeinschaft (DFG) to J.-R.N., grant NO110816 from the Innovative Medizinische Forschung (IMF) to J.-R.N. intramural resources of the Center for Laboratory Medicine to J.-R.N., FIRB-IDEAS grant RBID08777T from the Italian Ministry of Education, University and Research to J.-R.N. and M.S., and the Intramural Research Program of the National Institutes of Health, National Institute of Diabetes and Digestive and Kidney Disease to R.P.

ABSTRACT

Background: Sphingosine 1-phosphate (S1P) is a bioactive lysosphingolipid and a constituent of high density lipoprotein (HDL) exerting several atheroprotective effects *in vitro*. However, the few studies addressing anti-atherogenic effects of S1P *in vivo* have led to disparate results. We here examined atherosclerosis development in LDL-R-deficient (LDL-$R^{-/-}$) mice with elevated endogenous S1P levels. **Methods and Results**: Sublethally irradiated LDL-$R^{-/-}$ mice were transplanted with bone marrow (BM) deficient in sphingosine kinase 2 (SphK2), which led to elevation of S1P concentrations in erythrocytes, plasma, and HDL by approximately 1.5 – 2.0-fold in $SphK2^{-/-}$/LDL-$R^{-/-}$ mice. Afterwards, mice were fed a Western diet for 14 weeks. Elevation of endogenous S1P significantly reduced atherosclerotic lesion formation by approximately half without affecting plasma lipid profile. Furthermore, the macrophage content of atherosclerotic lesions and lipopolysaccharide (LPS)-induced monocyte recruitment to peritoneal cavity were reduced in $SphK2^{-/-}$/LDL-$R^{-/-}$ mice. Studies using intravital microscopy revealed that endogenous S1P lowered leukocyte adhesion to capillary wall and decreased endothelial permeability to fluorescently labeled LDL. Moreover, $SphK2^{-/-}$/LDL-$R^{-/-}$ mice displayed decreased levels of vascular cell adhesion molecule 1 (VCAM1) in atherosclerotic lesions and in plasma. Studies *in vitro* demonstrated reduced monocyte adhesion and transport across an endothelial layer exposed to increasing S1P concentrations, murine plasma enriched in S1P, or plasma obtained from SphK2-deficient animals. In addition, decreased permeability to fluorescence-labeled dextran beads or LDL was observed in S1P-treated endothelial cells. **Conclusion**: We conclude that raising endogenous S1P levels exerts anti-atherogenic effects in LDL-$R^{-/-}$ mice that are mediated by favorable modulation of endothelial function.

Key words: Sphingosine 1-phosphate (S1P), high density lipoproteins (HDL), sphingosine kinase 2 (SphK2), endothelial cells, atherosclerosis.

INTRODUCTION

Sphingosine 1–phosphate (S1P) is a membrane-derived sphingolipid that regulates diverse cellular processes including growth, survival, migration, angiogenesis, and inflammation [1,2]. S1P is synthesized intracellularly via phosphorylation of sphingosine by two distinct sphingosine kinases (SphK), SphK1 and SphK2, and was initially postulated to act as a second messenger [1,2]. Subsequent studies revealed that S1P is actively transported across the plasma membrane to the extracellular space, where it interacts with five cognate cell-surface receptors designated $S1P_{1-5}$ [3]. Though widely expressed, S1P receptors display tissue-specific distribution patterns with $S1P_1$, $S1P_2$ and $S1P_3$ being represented in vascular tissues. In endothelial cells S1P was found to promote adherence junction assembly resulting in the enhancement of endothelial barrier [4,5]. In addition, S1P decreased the expression of endothelial adhesion molecules such as vascular adhesion molecule 1 (VCAM1), and thereby abrogated the adhesion of monocytic cells to endothelial monolayer [6-8]. In smooth muscle cells, S1P suppressed the production of chemoattractant chemokines [8,9]. Consequently, S1P was postulated to exert anti-inflammatory effects by restricting the recruitment of leukocytes to sites of inflammation. Actually, lowering S1P concentration in plasma or defective expression of S1P receptors in endothelial cells exacerbated inflammatory response in murine models of ischaemia-reperfusion injury, acute lung injury, and anaphylaxis, while opposite effects were seen after restoration of plasma S1P levels or administration of S1P receptor agonists [1,4,10,11].

Erythrocytes, platelets, and endothelial cells are major sources of S1P in plasma, where it is mainly associated with an apolipoprotein M (apoM)-containing subfraction of high density lipoprotein (HDL) - a potent plasma-borne anti-atherogenic factor [1,4,12]. Growing evidence indicates that S1P accounts for a substantial portion of atheroprotective effects attributed to HDL. For instance, S1P closely correlates with

HDL in a concentration range, in which HDL most effectively protects against atherosclerosis, and decreased HDL-bound S1P levels were noted in patients with coronary artery disease and myocardial infarction [13-15]. Under *in vitro* condition, HDL-bound S1P was reported to mitigate endothelial apoptosis, stimulate nitric oxide and prostacyclin generation in endothelial and smooth muscle cells, inhibit expression of endothelial adhesion molecules, and produce persistent enhancement of endothelial barrier and reduction of vascular leak [16,17]. In addition, synthetic S1P mimetics such as FTY720 - a high affinity agonist for $S1P_{1,3,4,5}$ and KRP203 – a specific $S1P_1$ agonist diminished atherosclerotic lesions in LDL receptor-deficient (LDL-$R^{-/-}$) or apolipoprotein E-deficient (apo$E^{-/-}$) mice fed a high cholesterol diet, improved endothelial function by reducing leukocyte adhesion and suppressed inflammatory activation of macrophages [18-20]. More recently, cell-specific deletion of $S1P_1$ in endothelial cells or macrophages was shown to enhance atherosclerotic development in apo$E^{-/-}$ or LDL-$R^{-/-}$ mice, respectively [21,22]. By contrast, reduced vascular lesion formation was observed in apo$E^{-/-}$ mice deficient in $S1P_2$ or treated with synthetic $S1P_2$ antagonist [23]. Moreover, elevation of plasma S1P in apo$E^{-/-}$ mice overexpressing apoM augmented aortic root but not aortic arch atherosclerosis, and this effect was abolished under conditions of uremia [24]. Thus, the involvement of S1P in the atherosclerosis development appears to critically depend on the S1P receptor involved, the localization of lesions as well as the experimental setting, and anti-atherogenic effects of HDL-bound S1P remain controversial.

The objective of the present study was to assess the impact of endogenously synthesized S1P on the atherosclerotic lesion development. Our findings demonstrate that LDL-$R^{-/-}$ mice with hematopoietic SphK2 deficiency, which are characterized by elevated S1P levels in plasma, display attenuated development of atherosclerotic lesions, and attribute this beneficial effect to the enhancement of endothelial function.

MATERIAL AND METHODS

Animals – Generation of B6N.129S6-*Sphk2*^{tm1Rlp}/J mice deficient in SphK2 (SphK2$^{-/-}$) was described elsewhere [25]. Female LDL-R$^{-/-}$ mice (B6.129S7-*Ldlr*^{tm1Her}/J) were purchased from Jackson Laboratories, Bar Harbor, ME. Bone marrow (BM) aplasia was induced in LDL-R$^{-/-}$ mice (6-8 week of age) with a single dose of 11 Gy total body irradiation. Single-cell BM suspensions from SphK2$^{-/-}$ and wildtype (WT) mice were injected *i.v.* to irradiated recipients (5.0 x 10^6 cells/animal). The hematological chimerism of transplanted animals was determined in genomic DNA from blood leukocytes 4 weeks after transplantation. Thereafter, animals were put on Western diet (0.25% cholesterol, 21% fat; Altromin, Lage, Germany) for 14 weeks (assessment of atherosclerosis) or 4 weeks (assessment of endothelial function), sacrificed, and used for further analysis. All animal protocols used in this study conformed to national law and were approved by the animal protection authority (LANUV).

Lipid analysis and lipoprotein isolation and fractionation – Plasma total cholesterol (TC) and triglycerides (TG) were determined enzymatically (Siemens, Eschborn, Germany). Low and high-density lipoproteins (LDL, HDL) were isolated from plasma by a discontinuous gradient centrifugation. LDL was labeled with DyLight™ 594 fluorescent dye (DyL, Thermo Fischer, Schwerte, Germany) as recommended by the manufacturer. Plasma lipoproteins were fractionated using Smart™ chromatographic system (Pharmacia, Uppsala, Sweden) as described previously [19]. S1P concentrations were determined using liquid-chromatography tandem mass spectrometry as published previously [26].

Atherosclerotic lesion analysis – Hearts and proximal aortas were dissected and embedded in Tissue-Tek OCT. Atherosclerosis was assessed in aortic roots as described [18,27-29]. For *en face* analysis, Oil-Red-O-stained thoracic aorta was fixed between glass slides. Cross-sections for immunofluorescence microscopy were

stained with anti-mouse antibodies against monocytes/macrophages (MOMA-2) or VCAM1 and counterstained with 4',6-diamidino-2-phenylindole (DAPI, Thermo Fisher).

Assessment of leukocyte adhesion in vivo – Leukocyte adhesion *in vivo* was studied in anesthetized LDL-$R^{-/-}$ mice transplanted with $SphK2^{-/-}$ or WT BM. *In vivo* leukocyte staining was performed by intravenous injection of 1.0 µg/g rhodamine 6G (Sigma, Deisenhofen, Germany) and leukocyte adhesion was assessed by intravital microscopy of mesenterial venules using inverted fluorescence microscope (Eclipse 300, Nikon, Düsseldorf, Germany) as described previously [27].

Assessment of vascular permeability and monocyte recruitment – To assess vascular permeability, LDL-$R^{-/-}$ mice transplanted with $SphK2^{-/-}$ or WT BM were intravenously administered with Evans blue, fluorescein isothiocyanate (FITC)-dextran (500.0 kDa), or DyL-labeled LDL (DyL-LDL) 15 min prior to injection *i.p.* of lipopolysaccharide (LPS, 25 µg/animal), sacrificed after 3 h, and dye concentrations were measured in peritoneal lavage fluid by photometry or fluorescence spectrometry. For the assessment of monocyte recruitment to peritoneal cavity, LPS-injected animals were sacrificed after 18 h and monocytes/macrophages in the lavage fluid were stained with anti-F4/80 and anti-CD11b antibodies and counted using a FACSCalibur flow cytometer (BD Bioscience, San Jose, CA). Vascular permeability *in situ* was assessed in the ileal mesentery superfused with bradykinin (1.0 µg/mL). The DyL-LDL extravasation was monitored for 15 minutes by intravital microscopy and quantified using image analysis software ImageJ (NIMH, Bethesda, MD).

Determination of cytokine and adhesion molecule concentrations – Concentrations of cytokines and soluble adhesion molecules in plasma and cell supernatants were quantified by commercially available ELISAs (R&D Systems, Wiesbaden, Germany).

Endothelial adhesion and permeability assays – For the assessment of monocyte adhesion, U937 monocytes labeled with calcein-AM were added to confluent bEnd.5

murine endothelial cells on cover slip in a Dulbecco-modified Eagles medium (DMEM) supplemented with glutamine (2.0 %, v/v), sodium pyruvate (1.0 %, v/v), non-essential amino acids (1.0%, v/v), and endothelial cell growth supplement (Promocell, Heidelberg, Germany) containing epidermal growth factor (EGF), basic fibroblast growth factor (bFGF) and FCS (2.0 %, v/v). S1P (1.0 µmol/L or 2.0 µmol/L in some experiments) was added directly to cell culture media. The number of adherent cells was counted under fluorescence microscope Leica DM-IRE (Leica Mikrosysteme, Wetzlar, Germany). For endothelial permeability testing, bEnd.5 cells were seeded onto collagen-coated TransWell culture inserts (Corning Life Sciences, Lowell, MA) to form monolayers. FITC-dextran, DyL-LDL, or calcein-labeled U937 monocytes were placed in the apical insert compartment for 0.5 h or 4h. Samples were taken from basolateral chambers for fluorescence measurement.

Real-time quantitative RT-PCR - Total RNA was isolated from bEnd.5 murine endothelial cells using RNAeasy Plus Purification Kit (Qiagen, Hilden, Germany) and cDNA was synthesized by reverse transcription. Fully automated RT-PCR set-up was done on a Genesis 150 workstation (TECAN, Creilsheim, Germany) and PCR products were detected using ABI7900ht sequence detection system (Applied Biosystems, Darmstadt, Germany). Relative gene expression was calculated by applying the $2^{-\Delta\Delta Ct}$ method.

General Procedures - Data are presented as means ± S.D. for at least three separate experiments or as results representative of at least three repetitions. Comparisons between the means of two or multiple groups were performed with two-tailed Student t-test or one-way ANOVA for independent samples, respectively. Pairwise comparisons were performed with Student-Newman-Keuls post-hoc test. p values less than 0.05 were considered significant. Detailed Methods can be found online.

RESULTS

Hematopoietic SphK2 deficiency elevates plasma S1P level – SphK2-deficient mice display increased S1P concentrations in plasma [30]. To elevate plasma S1P levels in atherosclerosis-prone animals, sublethally irradiated LDL-R$^{-/-}$ mice were reconstituted with either SphK2$^{-/-}$ or WT BM. Analysis of SphK2$^{-/-}$ transplanted animals revealed that over 90% of blood cells were derived from SphK2$^{-/-}$ BM (Figure 1A). Body weight at sacrifice, plasma levels of total cholesterol and triglycerides as well as plasma lipid profiles were comparable between SphK2$^{-/-}$ and WT transplanted mice (Figure 1B and C). However, hematopoietic SphK2$^{-/-}$ deficiency led to an approximately 1.5 - 2-fold increase in S1P concentration in plasma and significantly raised the S1P content in erythrocytes (Figure 1D). In addition, SphK2 deficiency elevated the amount of S1P associated with HDL but not LDL or VLDL particles (Figure 1D).

Hematopoietic SphK2$^{-/-}$ chimeras show reduced atherosclerosis - To determine the effects of hematopoietic SphK2$^{-/-}$ deficiency on atherosclerosis development, Oil Red O-stained lesions in aortic root and thoracic aorta of Western diet-fed LDL-R$^{-/-}$ chimeras were analyzed. Morphometric quantification of atherosclerosis at the aortic root revealed that both absolute lesion size and the plaque-to-lumen ratio were significantly decreased in the SphK2$^{-/-}$ transplanted mice as compared to WT transplanted mice (Figure 2A). In addition, SphK2$^{-/-}$ chimeras displayed significantly smaller necrotic cores within aortic lesions. Analysis of e*n face* prepared thoracic aortas demonstrated a remarkable reduction of Oil Red O-positive lesions around branch ostia (Figure 2B). Immunohistochemical analysis of lesion composition in the aortic root yielded a significant reduction of MOMA-2-positive macrophage content in SphK2$^{-/-}$ chimeras as compared to WT transplanted controls (Figure 2C). By contrast, SphK2$^{-/-}$ chimerism did not affect the collagen content in the atherosclerotic lesions (not shown).

Hematopoietic SphK2 deficiency reduces leukocyte adhesion – As leukocyte-endothelial interactions represent a pivotal target of anti-atherogenic action of HDL-bound S1P, the influence of hematopoietic SphK2 deficiency on leukocyte was directly assessed *in vivo* in postcapillary venules. To this aim, leukocytes were intravitally labeled with fluorescence dye (rhodamine) in SphK2$^{-/-}$ and WT transplanted mice and cells adhering to the vascular wall were observed using intravital microscopy. We found that SphK2$^{-/-}$ chimerism substantially reduced leukocyte-endothelial interaction: the number of leukocytes rolling on vascular endothelium was significantly reduced in SphK2$^{-/-}$ transplanted LDL-R$^{-/-}$ mice as compared to controls and permanent adhesion showed a trend towards reduction (Figure 3A). Concomitantly, circulating levels of soluble isoforms of the endothelial adhesion molecule VCAM1 were significantly lower in plasma of SphK2$^{-/-}$ transplanted LDL-R$^{-/-}$ mice (Figure 3B). In addition, atherosclerotic lesions of SphK2$^{-/-}$ chimeras exhibited less expression of VCAM1 (Figure 3C).

To investigate *in vitro* correlates of anti-adhesive effects, which are exerted by elevated S1P in mice with hematopoietic SphK2 deficiency, bEnd.5 murine endothelial cells were pre-incubated with medium containing S1P in concentrations approximating those seen in WT and SphK2$^{-/-}$ transplanted mice (1.0 and 2.0 µmol/L, respectively). After 24 h cells were exposed to 100 U/mL of TNFα and the extent of U937 monocyte adhesion to the endothelium was examined using an *in vitro* cytoadherence assay, while the expression of endothelial adhesion molecules was determined by qPCR. As shown in Figure 3D and E, the adhesion of U937 monocytes to endothelial cells and the expression of VCAM1 were both reduced in a concentration-dependent fashion after pre-incubation with S1P. In addition, augmented downregulation of monocyte adhesion and VCAM1 expression was observed after pre-incubation of endothelial cells with WT mouse plasma enriched with S1P (1.0 µmol/L), or with plasma obtained

from SphK2-deficient mice (Figure 3D and E), indicating that the increment in S1P quantity in plasma is associated with augmentation of the inhibitory effects on monocyte adhesion.

Hematopoietic SphK2 deficiency enhances the endothelial barrier – Next, we assessed the effect of elevated S1P concentrations in hematopoietic SphK2 deficiency on the function of the endothelial barrier *in vivo*. To this purpose, alterations in vascular permeability were estimated by *i.v.* injection of Evans blue dye, which binds to serum proteins, high molecular weight FITC-dextran, or DyL-LDL, and quantification of the respective dye after 3 h in the peritoneal cavity of SphK2$^{-/-}$ and WT transplanted mice. Intraperitoneal injection of LPS produced a substantial influx of Evans blue, FITC-dextran, and DyL-LDL into the peritoneal cavity and each of these effects was substantially attenuated in SphK2$^{-/-}$ chimeras as compared to WT transplanted mice (Figure 4A). In addition, the effect of hematopoietic SphK2 deficiency on endothelial permeability for DyL-LDL was examined *in situ* in mesenterial capillaries observed with intravital microscopy. As shown in Figure 4B, DyL-LDL was entirely localized in capillaries both in SphK2$^{-/-}$ and WT transplanted mice, but underwent massive extravasation after exposure to bradykinin, which compromises the endothelial barrier and enhances the vascular permeability. Quantification of DyL-LDL in capillary vessels after bradykinin treatment revealed that significantly more DyL-LDL was retained intracapillarily in the in SphK2$^{-/-}$ chimeras as compared to WT transplanted mice (Figure 4B).

To investigate the influence SphK2$^{-/-}$ chimerism on monocyte capacity to migrate across the endothelial barrier, the recruitment of monocytes into peritoneal cavity was additionally examined in SphK2$^{-/-}$ and WT transplanted mice after *i.p.* injection of LPS. As shown in Figure 4C, accumulation of monocytes in the peritoneal cavity 18 h after LPS injection was significantly reduced in hematopoietic SphK2$^{-/-}$ deficiency.

To assess the effect of S1P on the function of the endothelial barrier *in vitro*, confluent bEnd.5 murine endothelial cells on TransWell culture inserts were exposed for 24 h to medium containing increasing S1P concentrations (1.0 or 2.0 µmol/L), WT mouse plasma enriched with S1P (1.0 µmol/L), or plasma obtained from SphK2-deficient or WT mice. Thereafter, endothelial permeability to FITC-dextran or DyL-LDL was determined. As shown in Figure 4D, increasing the exposure of endothelial cells to S1P consistently decreased the transfer of FITC-dextran or DyL-LDL across the endothelial monolayer irrespective of the exposure ambience. Similarly, migration of U937 monocytes across the endothelial monolayer was gradually inhibited by increasing S1P quantities (Figure 4D).

Hematopoietic SphK2 deficiency does not affect macrophage activation – Previous studies attributed anti-atherogenic effects exerted by S1P mimetics to the inhibition of macrophage activation and/or to alterations in T-cell distribution and function [18,19]. Therefore, we tested inflammatory responses in peritoneal macrophages isolated from SphK2$^{-/-}$ chimeras and WT transplanted mice. Both, basal and LPS-stimulated secretion of pro-inflammatory cyto- and chemokines (TNFα, MCP1, IL12p70) was comparable between SphK2$^{-/-}$ and WT macrophages, which also showed similar expression levels of MHC-II and CD86 – the surface markers of the pro-inflammatory macrophage activation (supplementary Figure IA) and similar monocyte blood count (supplementary Figure IC). Moreover, SphK2$^{-/-}$ chimerism exerted no effect on the lymphocyte count in blood and on CD4^{+} and CD8^{+} T-cell distribution in blood and spleen (supplementary Figure IB and C). Splenocytes obtained from SphK2$^{-/-}$ or WT transplanted mice showed similar response to concanavalin A (ConA) stimulation as assessed by determination of IL-2 and IFNγ concentrations in cell supernatants (supplementary Figure IB). In addition, comparable levels of macrophage- and T-cell-secreted pro-inflammatory cyto- and chemokines (TNFα, IFNγ, IL12p70, MCP1,

RANTES) were noted in plasmas from SphK2$^{-/-}$ chimeras and WT transplanted mice (supplementary Figure IC).

DISCUSSION

Several studies have demonstrated that synthetic S1P mimetics interacting with S1P receptor types present in vasculature exert anti-atherogenic effects in murine models of atherosclerosis [18-20]. Less effort, however, has been devoted towards understanding the relevance of endogenous S1P for the development of atherosclerotic lesions. We have previously reported reduced atherosclerosis in LDL-R$^{-/-}$ mice transplanted with bone marrow deficient in S1P degrading enzyme S1P lyase (Sgpl1), which are characterized by increased S1P levels in plasma [31]. While this finding was in principle consistent with atheroprotective effect exerted by endogenous S1P, the elevation of the plasma S1P concentration in Sgpl1$^{-/-}$ BM recipients was marginal (approx. 1.2-fold vs. control). By contrast, the hematopoietic Sgpl1 deficiency massively increased S1P content in the spleen and lymph nodes (over 100-fold vs. control), which led to disruption of S1P gradients between blood and lymphatic organs, produced severe lymphopenia and monocytosis, and profoundly affected T-cell and macrophage functions as evidenced by altered proliferation, migration and production of pro- and anti-inflammatory cytokines. In addition, Sgpl1$^{-/-}$ transplanted mice displayed significantly lower total cholesterol and triglycerides levels and less pro-atherogenic plasma lipoprotein profile with decreased cholesterol content in LDL and VLDL fractions. The pleiotropic phenotype seen in in Sgpl1$^{-/-}$ BM recipients made difficult to pinpoint the mechanism underlying the reduced atherosclerotic lesion formation observed in these animals. In the present study we took advantage of SphK2 deficient mice, which display a paradoxical increase in S1P concentrations in plasma and erythrocytes, but not in spleen and lymph nodes [26,30]. The latter effect likely arises because of the predominant involvement of SphK2 in the S1P release from red blood cells and its uptake by endothelial cells and lymphatic tissues rather than S1P production. Actually, impaired S1P transfer from erythrocytes to endothelial cells, but

not de novo S1P synthesis was previously observed in SphK2$^{-/-}$ animals [30]. In our hands, the transplantation of SphK2$^{-/-}$ bone marrow to LDL-R$^{-/-}$ led to a moderate, but significant increase of S1P level both in plasma and erythrocytes, but failed to produce overt monocytosis, lymphopenia or changes in CD4^{+} and CD8^{+} T-cell distribution in blood and lymphoid organs, which is concordant with previously published data [30]. In addition, plasma lipid levels and lipoprotein profiles were comparable between mice transplanted with WT and SphK2$^{-/-}$ BM. Notwithstanding, the elevation of plasma S1P levels in SphK2$^{-/-}$ chimeras was coupled to the significant reduction of both absolute and fractional area of atherosclerotic lesions in the aortic root and markedly attenuated accumulation of lipid-rich material around ostia of intercostal arteries, which represent areas of aorta predisposed to atherosclerosis. In addition, lesions seen in SphK2$^{-/-}$ transplanted LDL-R$^{-/-}$ mice showed reduced accumulation of macrophages, which are considered a culprit in atherosclerotic plaque buildup. Taken together, the present data strongly reinforce the notion that endogenous S1P in plasma exerts anti-atherogenic effects *in vivo.*

Both macrophages and T-cells are abundantly present throughout human and murine plaques and their interaction is required for the development of fully-fledged inflammation within the arterial wall [32,33]. Previous investigations exploiting synthetic S1P mimetics such as FTY720 or KRP203 suggested that the anti-atherogenic effects exerted by these compounds in murine models of atherosclerosis are at least partly related to lowering blood lymphocyte count and/or to reprogramming macrophages and CD4^{+} T-cells towards less inflammatory phenotypes (M2, Th2) [18,19]. However, the current study provides little evidence supporting the notion that similar mechanisms operate in case of elevation of endogenous S1P in plasma. Transplantation of SphK2$^{-/-}$ bone marrow to LDL-R$^{-/-}$ mice had no impact on blood leukocyte count. In addition, macrophages obtained from SphK2$^{-/-}$ chimeras showed normal expression of surface

activation markers (CD86, MHCII) and their response to proinflammatory stimulation was comparable with WT cells. The present findings agree with the data published by Xiong and colleagues, who failed to detect any differences between SphK2$^{-/-}$ and WT macrophages with respect to cellular proliferation and apoptosis as well as NFκB activation and cytokine expression and concluded that SphK2 is not required for inflammatory responses in macrophages [34]. However, the latter authors observed increased autophagy in macrophages deficient in SphK2. As autophagy is impaired in advanced stages of atherosclerosis and its absence promotes vascular lesion formation in part through activation of the inflammasome [35], it cannot be excluded that the enhancement of autophagy might additionally contribute to atheroprotective effects seen in the hematopoietic SphK2 deficiency.

Apart from dysregulation of innate and adaptive immune responses endothelial dysfunction represents an important component of the pathological process leading to development of atherosclerotic lesions. There is overwhelming evidence that plasma S1P is critically involved in the regulation of several endothelial functions relevant to the protection against atherosclerosis [4,8,16]. S1P, its synthetic mimetics, and compounds promoting endothelial expression of S1P receptors such as simvastatin were repeatedly demonstrated to downregulate TNFα-induced surface expression of the endothelial adhesion molecule VCAM1 under *in vitro* conditions and to suppress *ex vivo* monocyte adhesion to aortic explants [6,7,18,36,37]. As a consequence, administration of S1P receptor agonists to mice was effective in reducing the recruitment of monocytes into inflamed areas of heart, kidney, liver, and peripheral nerves and these effects were attributed to the immediate modulation of endothelial functions [38-42]. In addition, S1P has been firmly established as the single most potent plasma-born factor enhancing endothelial barrier integrity and interfering with S1P signaling was demonstrated to promote vascular leak, which could be ameliorated

by S1P mimetic administration [4,5]. Our present results substantially expand these previous findings in LDL-R$^{-/-}$ mice and provide several pieces of evidence suggesting that the endothelium represents a pivotal target of anti-atherogenic actions of endogenous S1P. First, perivital microscopic assessment of leukocyte-vessel wall interaction provided the first demonstration *in vivo* that raising S1P levels in plasma effectively suppresses leukocyte adhesion to endothelium, with the latter effect being likely dependent on the reduced expression of VCAM1. As a possible consequence of the impaired interaction between endothelial cells and leukocytes, reduced extravasation manifesting as a diminished presence of monocytes/macrophages in peritoneal cavities and atherosclerotic lesions was observed in SphK2$^{-/-}$ chimeras. Second, the elevation of endogenous S1P in SphK2$^{-/-}$ chimeras effectively enhanced the endothelial barrier as evidenced by the reduced influx of molecular indicators such as Evans blue or FITC-dextran into the peritoneal cavity. Even more important from the perspective of atherosclerotic plaque pathology and for the first time demonstrated by the present study was a sharp reduction of vascular permeability for LDL in SphK2$^{-/-}$ chimeras, which likely translated into abated lipid deposition around intercostal artery ostia in the descending thoracic aorta. Third, the beneficial effects exerted by endogenous S1P on endothelial functions in mice could be entirely recapitulated using an *in vitro* approach, which closely emulated incremental increases in S1P concentrations occurring as a result of SphK2$^{-/-}$ bone marrow transplantation. Collectively, our findings suggest that endogenous S1P favorably affects several endothelial functions relevant to the pathogenesis of atherosclerosis, which culminates in the reduced penetration of both monocytes and LDL particles into the arterial wall. As both, monocyte and LDL retention in the subendothelial space, followed by the ingestion of LDL by intimal macrophages constitute crucial steps in the formation of atherosclerotic lesions, we hypothesize that these effects predominantly account for

the anti-atherogenic effects of endogenous S1P seen in hematogenous SphK2 deficiency.

S1P is carried in plasma by the apoM-containing subfraction of HDL with the remainder being associated with albumin and LDL [1,2,12]. As elevation of S1P level in plasma after SphK2$^{-/-}$ bone marrow transplantation likely arose as a consequence of the enhanced release from S1P-enriched erythrocytes, our results do not allow us to attribute the favorable effects on endothelial function observed in SphK2$^{-/-}$ chimeras specifically to HDL-bound S1P. However, the increased amount of S1P associated with HDL, but not LDL or VLDL in these animals is consistent with the notion that these lipoproteins might serve as a preferential acceptor for S1P liberated from erythrocytes, particularly as apoM-containing HDL has been recently identified as a principal mediator of S1P efflux from human red cells [43]. In this context, it is worth noticing that HDL-bound S1P has been previously identified to act as a biased agonist for $S1P_1$ [21]. Actually, HDL-bound S1P was found to most effectively promote the $S1P_1$- and β-arrestin-2-dependent signaling in endothelial cells and thereby to prevent TNFα-induced NF-κB activation and adhesion molecule expression. Conversely, apoM-deprived HDL, which contains negligible amounts of S1P, was demonstrated to lose its favorable effects on the endothelial functions, which were severely impaired in apoM-deficient mice [44-46]. In our experimental setting *in vitro* S1P was added to cell culture medium containing traces of lipoproteins, which might additionally facilitate its beneficial effects on endothelial cells. Taking these into account, it would be tempting to speculate that HDL assumes an important role in mediating the protective effects of S1P on endothelial function and against atherosclerosis, which are observed in LDL-R$^{-/-}$ mice transplanted with SphK2$^{-/-}$ bone marrow.

In conclusion, our study documents for the first time that raising endogenous S1P levels in LDL-R$^{-/-}$ mice exerts anti-atherogenic effects and that vascular endothelium

represents the major target of the atheroprotective effects exerted by S1P. Further research efforts will be necessary to delineate the molecular mechanisms responsible for the beneficial action of S1P and to identify the relevant S1P receptors.

ACKNOWLEDGEMENTS

The expert technical assistance of Beate Schulte and Cornelia Richter-Elsenheimer is gratefully acknowledged.

CONFLICT OF INTEREST

None.

REFERENCES

1. Proia RL, Hla T. Emerging biology of sphingosine-1-phosphate: its role in pathogenesis and therapy. J Clin Invest. 2015;125:1379-87
2. Pyne S, Adams DR, Pyne NJ. Sphingosine 1-phosphate and sphingosine kinases in health and disease: Recent advances. Prog Lipid Res. 2016;62:93-106
3. Blaho VA, Hla T. Regulation of mammalian physiology, development, and disease by the sphingosine 1-phosphate and lysophosphatidic acid receptors. Chem Rev. 2011;111:6299-320
4. Xiong Y, Hla T. S1P control of endothelial integrity. Curr Top Microbiol Immunol. 2014;378:85-105
5. Wilkerson BA, Argraves KM. The role of sphingosine-1-phosphate in endothelial barrier function. Biochim Biophys Acta. 2014;1841:1403-1412
6. Bolick DT, Srinivasan S, Kim KW, et al. Sphingosine-1-phosphate prevents tumor necrosis factor-α-–mediated monocyte adhesion to aortic endothelium in mice. Arterioscler. Thromb. Vasc. Biol. 2005;25:976–81
7. Kimura T, Tomura H, Mogi C, et al. Role of scavenger receptor class B type I and sphingosine 1-phosphate receptors in high density lipoprotein-induced inhibition of adhesion molecule expression in endothelial cells. J. Biol. Chem. 2006;281:37457–67
8. Schuchardt M, Tölle M, Prüfer J, et al. Pharmacological relevance and potential of sphingosine 1-phosphate in the vascular system. Br J Pharmacol. 2011;163:1140-62
9. Tölle M, Pawlak A, Schuchardt M, et al. HDL-associated lysosphingolipids inhibit NAD(P)H oxidase-dependent monocyte chemoattractant protein-1 production. Arterioscler Thromb Vasc Biol. 2008;28:1542-8

10. Karliner JS. Sphingosine kinase and sphingosine 1-phosphate in the heart: a decade of progress. Biochim Biophys Acta. 2013;1831:203-12
11. Abbasi T, Garcia JG. Sphingolipids in lung endothelial biology and regulation of vascular integrity. Handb Exp Pharmacol. 2013;216:201-26
12. Christoffersen C, Nielsen LB. Apolipoprotein M: bridging HDL and endothelial function. Curr Opin Lipidol. 2013;24:295-300
13. Karuna R, Park R, Othman A, et al. Plasma levels of sphingosine-1-phosphate and apolipoprotein M in patients with monogenic disorders of HDL metabolism. Atherosclerosis. 2011;219:855-63
14. Argraves KM, Sethi AA, Gazzolo PJ, et al. S1P, dihydro-S1P and C24:1-ceramide levels in the HDL-containing fraction of serum inversely correlate with occurrence of ischemic heart disease. Lipids Health Dis. 2011;10:70.
15. Sattler K, Gräler M, Keul P, et al. Defects of High-Density Lipoproteins in Coronary Artery Disease Caused by Low Sphingosine-1-Phosphate Content: Correction by Sphingosine-1-Phosphate-Loading. J Am Coll Cardiol. 2015;66:1470-85
16. Potì F, Simoni M, Nofer JR. Atheroprotective role of high-density lipoprotein (HDL)-associated sphingosine-1-phosphate (S1P). Cardiovasc Res. 2014;103:395-404
17. Levkau B. HDL-S1P: cardiovascular functions, disease-associated alterations, and therapeutic applications. Front Pharmacol. 2015;6:243.
18. Potì F, Gualtieri F, Sacchi S, et al. KRP-203, sphingosine 1-phosphate receptor type 1 agonist, ameliorates atherosclerosis in LDL-R−/− mice. Arterioscler Thromb Vasc Biol. 2013;33:1505–12.
19. Nofer JR, Bot M, Brodde M, et al. FTY720, a synthetic sphingosine 1 phosphate analogue, inhibits development of atherosclerosis in low-density lipoprotein receptor–deficient mice. Circulation. 2007;115:501–8.

20. Keul P, Tölle M, Lucke S, et al. The sphingosine-1-phosphate analogue FTY720 reduces atherosclerosis in apolipoprotein E–deficient mice. Arterioscler Thromb Vasc Biol. 2007;27:607–13
21. Galvani S, Sanson M, Blaho VA, et al. HDL-bound sphingosine 1-phosphate acts as a biased agonist for the endothelial cell receptor S1P1 to limit vascular inflammation. Sci Signal. 2015;8:ra79
22. Gonzalez L, Qian AS, Tahir U, et al. Sphingosine-1-Phosphate Receptor 1, Expressed in Myeloid Cells, Slows Diet-Induced Atherosclerosis and Protects against Macrophage Apoptosis in Ldlr KO Mice. Int J Mol Sci. 2017;18(12). pii: E2721
23. Skoura A, Michaud J, Im DS, et al. Sphingosine-1-phosphate receptor-2 function in myeloid cells regulates vascular inflammation and atherosclerosis. Arterioscler Thromb Vasc Biol. 2011;31:81-5
24. Bosteen MH, Madsen Svarrer EM, et al. Effects of apolipoprotein M in uremic atherosclerosis. Atherosclerosis. 2017;265:93-101
25. Mizugishi K, Yamashita T, Olivera A, et al. Essential role for sphingosine kinases in neural and vascular development. Mol Cell Biol 2005;25:11113-21
26. Ceglarek U, Dittrich J, Helmschrodt C, et al. Preanalytical standardization of sphingosine-1-phosphate, sphinganine-1-phosphate and sphingosine analysis in human plasma by liquid chromatography-tandem mass spectrometry. Clin Chim Acta. 2014;435:1-6
27. Poti F, Bot M, Costa S, et al. Sphingosine kinase inhibition exerts both pro- and anti-atherogenic effects in low-density lipoprotein receptor-deficient (LDL-R(-/-)) mice. Thromb Haemost. 2012;107:552-61.

28. Eschert H, Sindermann JR, Scheld HH, et al. Vascular remodeling in ApoE-deficient mice: diet dependent modulation after carotid ligation. Atherosclerosis. 2009;204:96-104
29. Nitschke Y, Weissen-Plenz G, Terkeltaub R, et al. Npp1 promotes atherosclerosis in ApoE knockout mice. J Cell Mol Med. 2011;15:2273-83
30. Sensken SC, Bode C, Nagarajan M, et al. Redistribution of sphingosine 1-phosphate by sphingosine kinase 2 contributes to lymphopenia. J Immunol. 2010;184:4133-42
31. Bot M, Van Veldhoven PP, de Jager SC, et al. Hematopoietic sphingosine 1-phosphate lyase deficiency decreases atherosclerotic lesion development in LDL-receptor deficient mice. PLoS One. 2013;8:e63360
32. Moore KJ, Sheedy FJ, Fisher EA. Macrophages in atherosclerosis: a dynamic balance. Nat Rev Immunol. 2013;13:709-21
33. Hedrick CC. Lymphocytes in atherosclerosis. Arterioscler Thromb Vasc Biol. 2015;35:253-7
34. Xiong Y, Lee HJ, Mariko B, et al. Sphingosine kinases are not required for inflammatory responses in macrophages. J Biol Chem. 2013;288:32563-73
35. Maiuri MC, Grassia G, Platt AM, et al. Macrophage autophagy in atherosclerosis. Mediators Inflamm. 2013;2013:584715
36. Kimura T, Tomura H, Mogi C, et al. Sphingosine 1-phosphate receptors mediate stimulatory and inhibitory signalings for expression of adhesion molecules in endothelial cells. Cell Signal. 2006;18:841–50
37. Kimura T, Mogi C, Tomura H, et al. Induction of scavenger receptor class B type I is critical for simvastatin enhancement of high-density lipoprotein-induced anti-inflammatory actions in endothelial cells. J Immunol. 2008;181:7332-40

38. Shimizu H, Takahashi M, Kaneko T, et al. KRP-203, a novel synthetic immunosuppressant, prolongs graft survival and attenuates chronic rejection in rat skin and heart allografts. Circulation. 2005;111:222-9
39. Kaneko T, Murakami T, Kawana H, et al. Biochem Biophys Res Commun. Sphingosine-1-phosphate receptor agonists suppress concanavalin A-induced hepatic injury in mice. Biochem Biophys Res Commun 2006;345:85-92
40. Ogawa R, Takahashi M, Hirose S, et al. A novel sphingosine-1-phosphate receptor agonist KRP-203 attenuates rat autoimmune myocarditis. Biochem Biophys Res Commun. 2007;361:621-8.
41. Zhang ZY, Zhang Z, Zug C, et al. AUY954, a selective S1P(1) modulator, prevents experimental autoimmune neuritis. J Neuroimmunol. 2009;216:59-65
42. Bajwa A, Jo SK, Ye H, et al. Activation of sphingosine-1-phosphate 1 receptor in the proximal tubule protects against ischemia-reperfusion injury. J Am Soc Nephrol. 2010;21:955-65
43. Christensen PM, Bosteen MH, Hajny S, et al. Apolipoprotein M mediates sphingosine-1-phosphate efflux from erythrocytes. Sci Rep. 2017;7:14983
44. Christensen PM, Liu CH, Swendeman SL, et al. Impaired endothelial barrier function in apolipoprotein M-deficient mice is dependent on sphingosine-1-phosphate receptor 1. FASEB J. 2016;30:2351-9
45. Ruiz M, Frej C, Holmér A, et al. High-Density Lipoprotein-associated apolipoprotein M limits endothelial inflammation by delivering sphingosine-1-phosphate to the sphingosine-1-phosphate receptor 1. Arterioscler Thromb Vasc Biol. 2017;37:118-129
46. Ruiz M, Okada H, Dahlbäck B. HDL-associated ApoM is anti-apoptotic by delivering sphingosine 1-phosphate to S1P1 & S1P3 receptors on vascular endothelium. Lipids Health Dis. 2017;16:36

LEGENDS TO FIGURES

***Figure 1**. Hematopoietic SphK2 deficiency elevates endogenous S1P levels* - LDL-R$^{-/-}$ mice transplanted with SphK2$^{-/-}$ (n=11) or WT (n=11) BM were placed on a Western-type diet for 14 weeks and sacrificed by exsanguination. **A**. BM repopulation was assessed by PCR. **B**. Body weight at sacrifice. **C**. Total cholesterol and triglycerides in plasma were determined by routine laboratory methods. Right panel: Plasma lipoprotein profile obtained by FPLC in SphK2$^{-/-}$ (○) or WT (■) transplanted animals. **D**. S1P was determined in erythrocytes, plasma, or lipoprotein fractions by mass spectrometry as described in Material and Methods. * - $p<0.05$, ** - $p<0.01$ (SphK2$^{-/-}$ vs. WT).

***Figure 2**. Hematopoietic SphK2 deficiency attenuates atherosclerotic lesion development in LDL-R$^{-/-}$ mice* - Aortic root and thoracic aortas obtained from Western-type diet-fed LDL-R$^{-/-}$ mice transplanted with SphK2$^{-/-}$ (n=11) or WT (n=11) BM were fixed, stained and used for morphometric analysis or stained for macrophages (MOMA-2). **A.** Representative Oil Red O stainings of aortic root lesions from SphK2$^{-/-}$ or WT chimeras and quantification of atherosclerotic lesion area, intima/lumen ratio, and necrotic core area (bar graphs). **B**. Representative photomicrographs of oil-red O stained “en face” prepared thoracic aorta and quantification of the lipid infiltration area (bar graph). **C**. Fluorescence photomicrographs showing MOMA-2 staining (red) from SphK2$^{-/-}$- or WT-transplanted mice. Blue fluorescence – counterstaining with DAPI. Bar graph shows the content of macrophages in the atherosclerotic plaque expressed as the percentage of intimal area. * - $p<0.05$, ** - $p<0.01$, *** - $p<0.001$ (SphK2$^{-/-}$ vs. WT).

***Figure 3**. Hematopoietic SphK2 deficiency reduces leukocyte adhesion in LDL-R$^{-/-}$ mice* – **A**. Tethering and adherence of perivitally labeled leukocytes to capillary vessel wall was examined in Western-type diet-fed LDL-R$^{-/-}$ mice transplanted with SphK2$^{-/-}$ (n=6) or WT (n=6) BM using intravital microscopy. Left panel: Representative video

snapshots of rolling/sticking cells in mesenterial arterioles. Arrows indicate fluorescently labeled adherent leukocytes. Right panel – bar graph showing quantification of rolling and sticking leukocytes. **B**. Bar graph demonstrating VCAM1 concentrations in plasmas obtained from SphK2$^{-/-}$- or WT-transplanted LDL-R$^{-/-}$ mice (n=11 per group). **C**. Fluorescence photomicrographs showing VCAM1 staining (green fluorescence) in aortic roots obtained from SphK2$^{-/-}$ or WT chimeras (both n=11). Blue fluorescence – counterstaining with DAPI. Bar graph shows the quantification of VCAM1 in atherosclerotic lesions expressed as the percentage of intimal area. * - $p<0.05$, ** - $p<0.01$ (SphK2$^{-/-}$ vs. WT). **D.** bEnd.5 murine endothelial cells pretreated for 24h with S1P (1.0 or 2.0 µmol/L, left bar graph), WT plasma enriched with S1P (1.0 µmol/L, center bar graph) or plasma obtained from SphK2$^{-/-}$ mice (right bar graph) were stimulated with TNFα (50.0 ng/mL) for 4 h. The adherence of calcein-loaded U937 monocytes was evaluated under a fluorescence microscope. **E**. bEnd.5 cells pretreated as described above were examined for VCAM-1 expression using qPCR. Data are representative for 3 to 5 independent experiments. * - $p<0.05$, ** - $p<0.01$ (as indicated in the figure).

Figure 4*. Hematopoietic SphK2 deficiency reduces endothelial permeability in LDL-R$^{-/-}$ mice* – Western-type diet-fed LDL-R$^{-/-}$ mice transplanted with SphK2$^{-/-}$ or WT BM were injected with Evans blue (600 µg/animal), FITC-dextran (500 µg/animal) or DyL-LDL (500 µg/animal) **A.** Following to *i.p.* injection of LPS (25 µg/animal) peritoneal cavity was washed and concentrations of respective dyes were determined as described in Material and Methods. Shown are data from two independent experiments with 5 – 6 animals/group in experiment. **B**. Mice ileal mesentery was superfused with bradykinin (1.0 µg/mL), and DyL-LDL was monitored for 15 minutes by intravital microscopy. Left panel - original photographs of mesenterial arterioles. Right panel – bar graph showing quantification of intravasal DyL-LDL in SphK2$^{-/-}$ and WT chimeras (both n=6). **C**. Bar

graph showing quantification of monocytes in peritoneal cavity of SphK2$^{-/-}$ (n=5) and WT (n=6) chimeras following to *i.p.* injection of LPS (25 µg/animal). * - $p<0.05$, ** - $p<0.01$ (SphK2$^{-/-}$ vs. WT). **D**. bEnd.5 murine endothelial cells in TransWell inserts were exposed for 24h to S1P (1.0 or 2.0 µmol/L, left bar graphs), WT plasma enriched with S1P (1.0 µmol/L, center bar graphs) or plasma obtained from SphK2$^{-/-}$ mice (right bar graphs). FITC-dextran, DyL-LDL or calcein-loaded U937 cells were placed in the apical compartment of the insert and the influx or migration across the endothelial layer was quantified by determining fluorescence in the basolateral compartment. Results are expressed as the percentage of influx/migration across untreated monolayers. Data are representative for 3 to 5 independent experiments. * - $p<0.05$, ** - $p<0.01$ (as indicated in the figure).

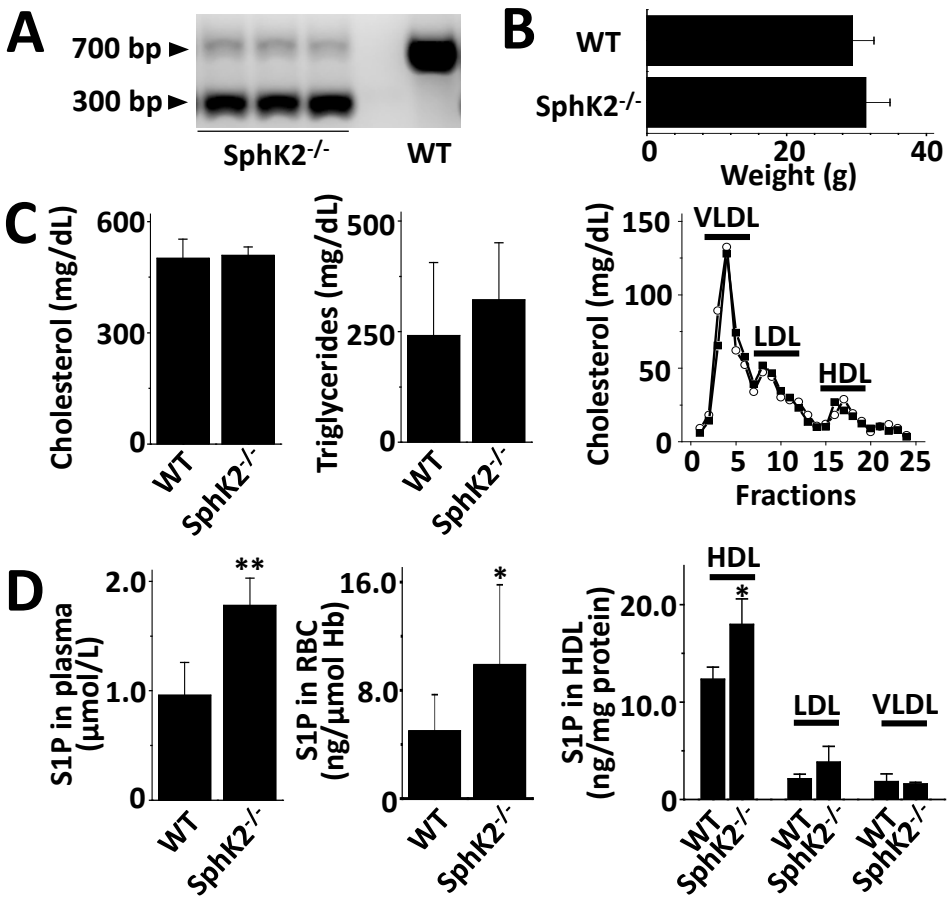

Feuerborn et al. Fig. 1

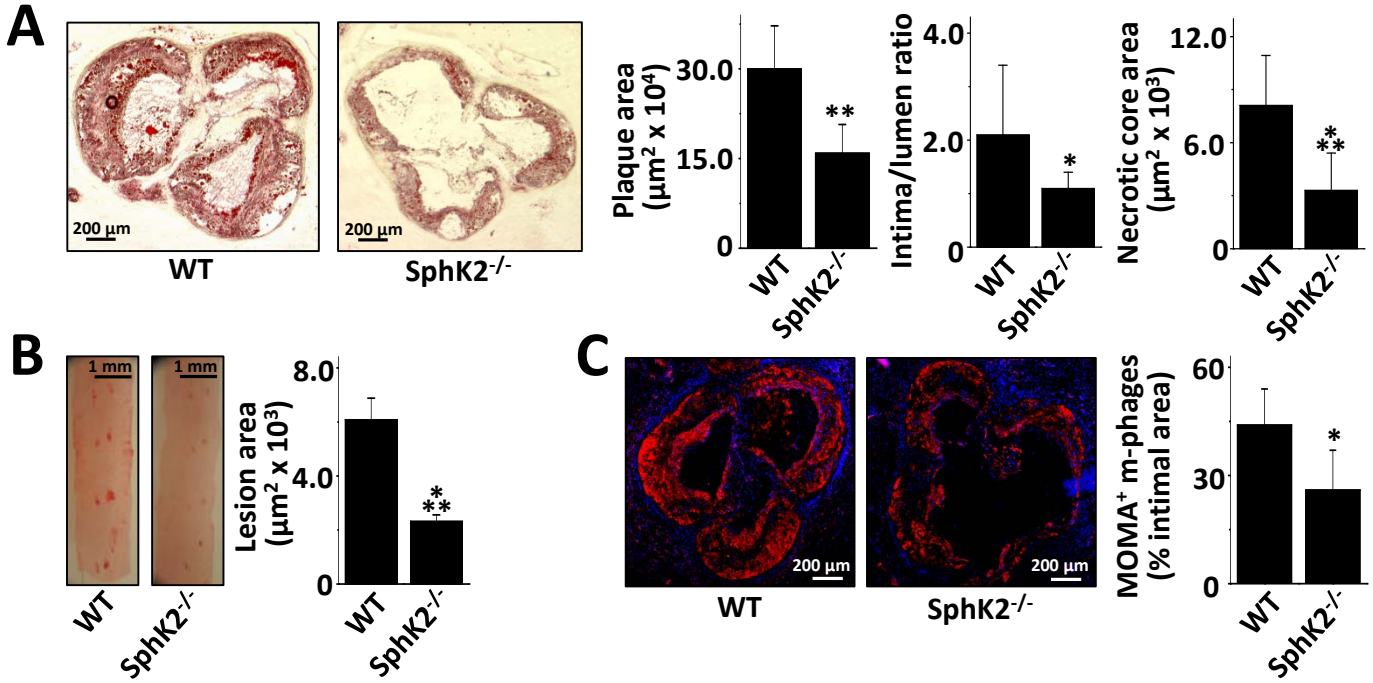

Feuerborn et al. Fig. 2

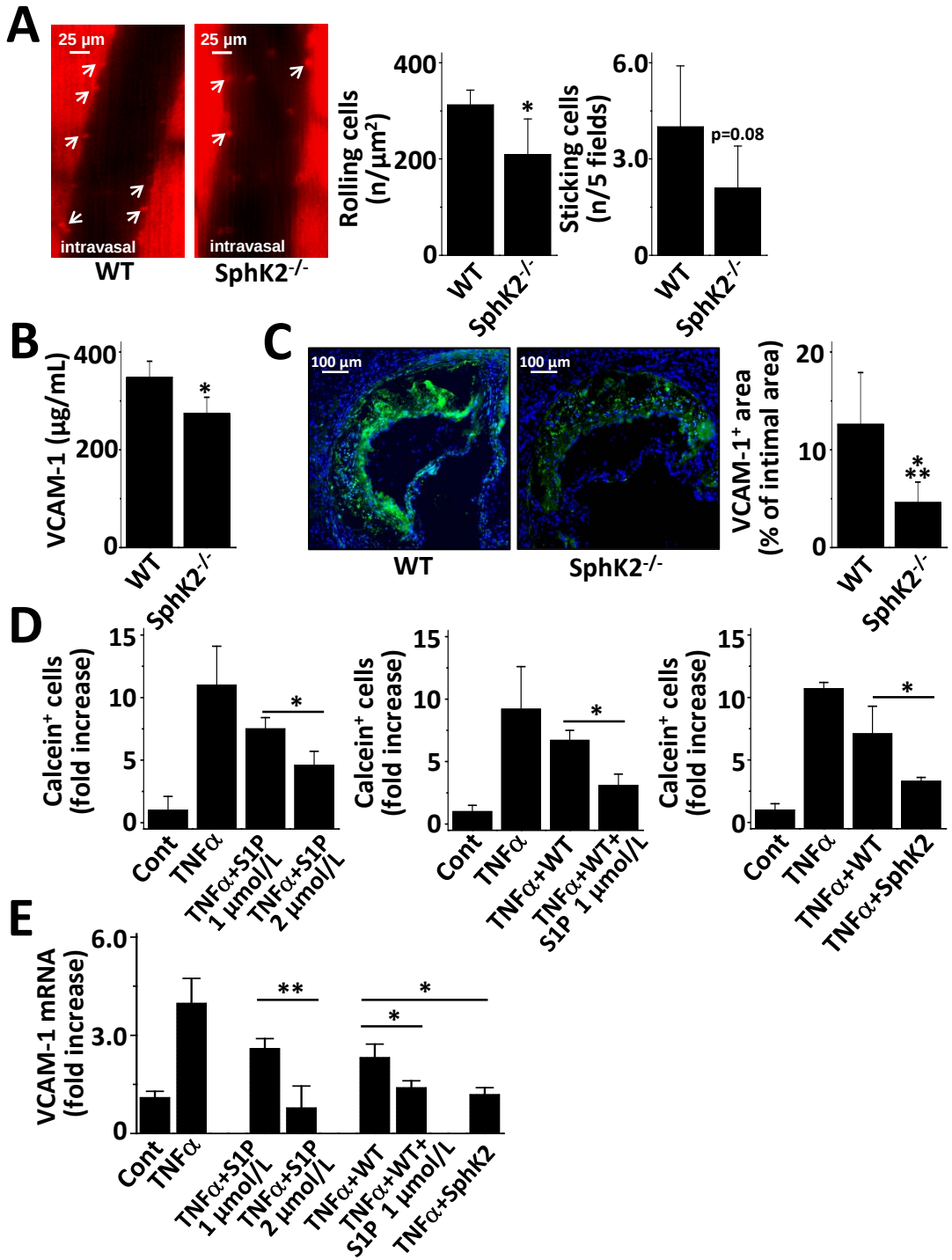

Feuerborn et al. Fig. 3

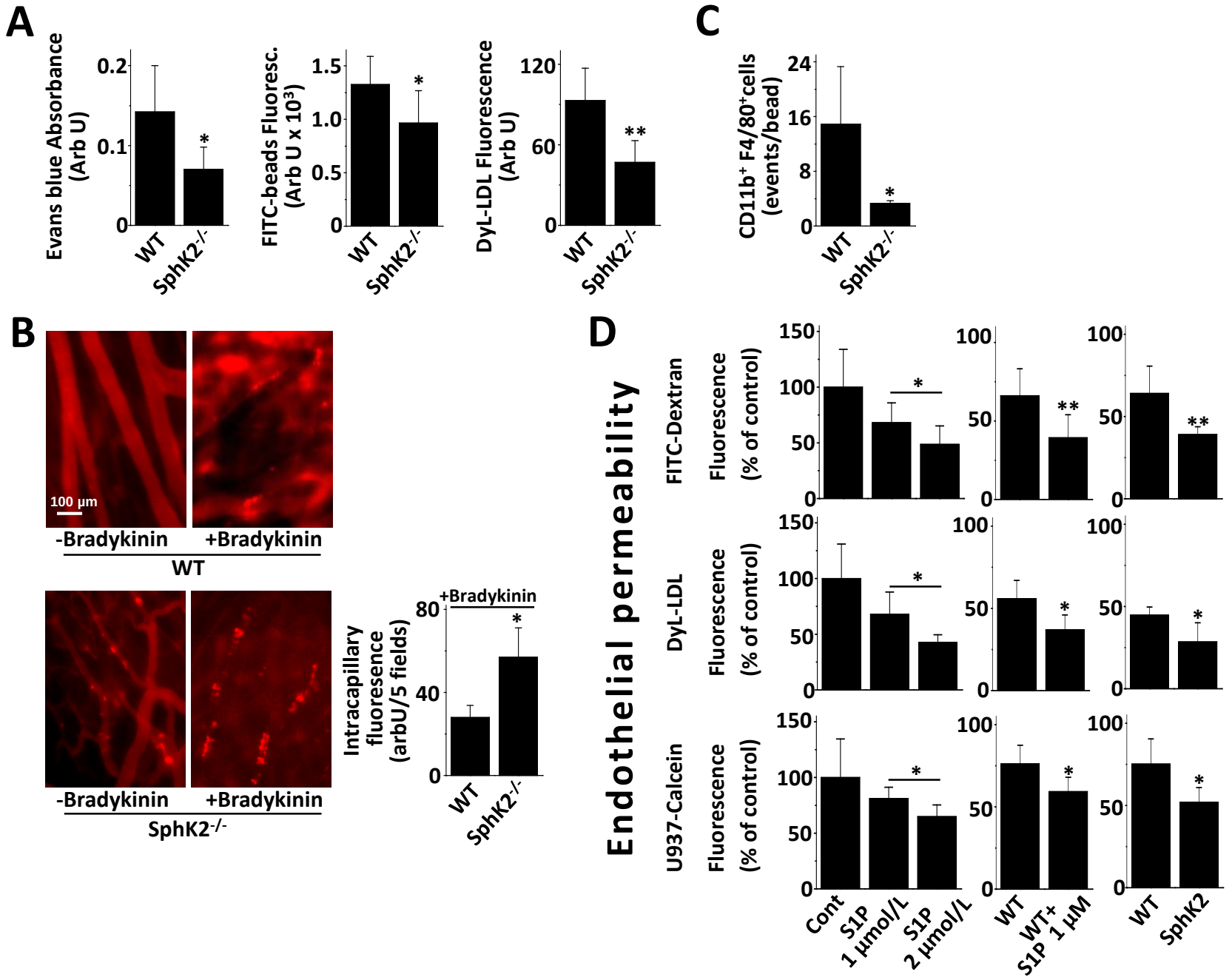

Feuerborn et al. Fig. 4

FEUERBORN et al.: ELEVATING ENDOGENOUS SPHINGOSINE 1-PHOSPHATE (S1P) LEVELS IN PLASMA IMPROVES ENDOTHELIAL FUNCTION AND AMELIORATES ATHEROSCLEROSIS IN LDL-R$^{-/-}$ MICE

SUPPLEMENTAL MATERIAL

MATERIAL AND METHODS

Animals – B6N.129S6-*Sphk2*^{tm1Rlp}/J mice, in which part of exon 4 and exons 5-7 of the sphingosine kinase 2 (Sphk2) gene was replaced by a β-galactosidase (*lacZ*)-neomycin resistance (neo) cassette abolishing gene function, was generated as described previously [1]. Female LDL-R$^{-/-}$ mice on a C57BL/6J background (B6.129S7-*Ldlr*^{tm1Her}/J) were purchased from Jackson Laboratories, Bar Harbor, ME. To induce bone marrow aplasia, LDL-R$^{-/-}$ mice (6-8 week of age) were exposed to a single total dose of 11 Gy total body irradiation 1 day before the transplantation. Bone marrow (BM) was isolated by flushing femurs and tibias from female SphK2$^{-/-}$ and WT mice with phosphate-buffered saline (PBS) and single-cell suspensions were prepared by passing the cells through a 70 µm cell strainer. Irradiated recipients received 5.0 x 10^6 cells by intravenous injection into the tail vein. The hematological chimerism of transplanted animals was determined in genomic DNA from blood leukocytes 4 weeks after transplantation. Thereafter, animals were put on the Western diet (0.25% cholesterol, 21% fat; Altromin, Lage, Germany) for 14 weeks (assessment of atherosclerosis) or 2 - 4 weeks (assessment of endothelial function). At the end of the treatment period mice were sacrificed by exsanguination by heart puncture or cervical dislocation under anesthesia and tissues were collected for further analysis. All animal experiments were approved by government authorities in charge of animal protection (LANUV).

Low density lipoprotein (LDL) isolation and labeling – Low density lipoprotein (LDL) was isolated from the pooled plasma of healthy blood donors by a discontinuous potassium bromide gradient centrifugation (d=1.125-1.210 g/mL). LDL was labeled with DyLight™ 594 fluorescent dye (DyL, Thermo Fischer, Schwerte, Germany) according to the manufacturer instruction. Briefly, LDL (2.0 mg/mL, pH adjusted to 8.0 with 50 mmol/L sodium borate) was mixed with DyLight™ 594 reagent (1:1, v/v), incubated for 60 min, and purified using spin columns provided by the manufacturer. The labeling efficiency was assessed by fluorescence spectroscopy.

Lipid analysis and lipoprotein fractionation – Plasma total cholesterol (TC), HDL-cholesterol (HDL-C) and triglycerides (TG) were determined enzymatically using commercially available kits (Siemens, Eschborn, Germany). Plasma lipoproteins were fractionated using Smart™ chromatographic system (Pharmacia, Uppsala, Sweden) as described previously [2]. HDL was isolated from mouse plasma by discontinuous ultracentrifugation. S1P concentrations in murine plasma and HDL were determined using hydrophilic interaction liquid chromatography (HILIC, SeQuant™ ZIC®-HILIC column) followed by tandem mass spectrometry as published previously [3].

Atherosclerotic lesion analysis – Assessment of atherosclerotic lesion size and cellularity was performed as described previously [4-6]. Briefly, exsanguinated mice were subjected to *in situ* perfusion with saline through the left cardiac ventricle. For analysis of spontaneous atherosclerosis aortic roots were removed and embedded in OCT-kryoprotective medium. Serial cross-sections were collected, stained with Oil-Red-O for lipid and counterstained with hematoxilin (Sigma). Atherosclerotic lesion size at the aortic root was determined as the mean of 5 Oil-Red-O-stained sections through the aortic valve area, each section 50 µm apart from each other. For *en face* analysis, the thoracic aorta was opened longitudinally, Oil-Red-O-stained and fixed between glass slides. Images were digitally captured with a Leica DM-LB microscope

equipped with JVC KY-F75 color camera (Leica Microsystems, Wetzlar, Germany). The extent of atherosclerosis was quantified by computerized image analysis using Leica Qwin image analysis software. Lesion size was expressed as stained area (μm^2) or as percentage ratio between the area occupied by atherosclerotic plaque and the total area of aorta. For immunochemistry, aortic root sections were stained with antibodies directed against mouse macrophages (rat anti-mouse MOMA-2, 1:100, Millipore), vascular smooth muscle cell (rat anti-mouse actin, Sigma), or VCAM1 (1:400, rabbit anti-mouse VCAM, Abbiotec, San Diego). For labeling, secondary goat anti-rat and goat anti-rabbit antibodies conjugated to Cy3 (1:500; Dianova, Hamburg) or to AlexaFluor® 488 (1:200; MoBiTec, Göttingen) were used. Following incubation conditions were used: primary antibodies at 4°C overnight, secondary antibodies at RT for 1 h. Some sections were counterstained with 4',6-diamidino-2-phenylindole (DAPI, Thermo Fisher) for nuclear morphology. Negative controls were performed by omitting primary antibodies. Images were analyzed using a a AXIOPHOT2™ fluorescence microscope (Zeiss, Jena, Germany) and positive areas were quantified using the image analysis software ImageJ (National Institute of Health, Bethesda, MD, USA).

Assessment of leukocyte adhesion in vivo – For studying leukocyte adhesion under *in vivo* conditions, LDL-$R^{-/-}$ mice transplanted with $SphK2^{-/-}$ or WT BM were subjected to inhalation anesthesia using isoflurane (minimum alveolar concentration (MAC) 1.5 Vol. %). *In vivo* leukocyte staining was performed by intravenous injection of 1.0 µg/g rhodamine 6G (Sigma, Deisenhofen, Germany) and leukocyte adhesion was assessed by intravital microscopy of mesenterial venules as described previously [7]. For this purpose, a small midline laparotomy was made in the lower abdomen, animals were placed on a prewarmed inverted fluorescence microscope (Eclipse 300, Nikon, Düsseldorf, Germany) and a part of the distal ileum was gently exteriorized on a slide in a tension free position. To avoid dehydration and hypothermia, the tissue was

covered with a coverslip and continuously moistured with warmed phosphate buffered saline (pH 7.4). In each animal, visual fields of 5 non-branched mesenteric venules (60-140 µm diameters) were analyzed and recorded for 30 sec by a fluorescence camera (FView II Olympus Soft Imaging Systems, Münster, Germany). Fluorescent cells moving in close contact along the endothelium at a velocity less than that of free floating cells are considered to be rolling leukocytes. Permanently adherent cells were defined to remain stationary for more than 20 sec. The numbers of leukocytes were normalized on 1 mm^2 venular surface area.

Assessment of vascular permeability and monocyte recruitment – To assess vascular permeability, LDL-$R^{-/-}$ mice transplanted with SphK2$^{-/-}$ or WT BM were intravenously administered with Evans blue (600 µg/animal), fluorescein isothiocyanate (FITC)-dextran (Sigma, 500 kDa; 500 µg/animal), or DyL-LDL (500 µg/animal) 15 min prior to injection *i.p.* of LPS (25 µg/animal). Mice were sacrificed after 3 h and their peritoneal cavities were washed with 10 mL of ice-cold heparinized PBS. The cells were spun down and the supernatants were analyzed for Evans blue with photometry (620 nm, FluoStar Optima, BMG LabTech, Ortenberg, Germany) and for FITC-dextran or DyL-LDL with fluorescence spectrometry (ex/em 485 nm/520 nm or 560 nm/590 nm, respectively, FluoStar Optima). For the assessment of monocyte recruitment to peritoneal cavity, LDL-$R^{-/-}$ mice transplanted with SphK2$^{-/-}$ or WT BM were administered *i.p.* with LPS (25 µg/animal). LPS-injected animals were sacrificed after 18 h and peritoneal cavities were washed with 10 mL of ice-cold heparinized PBS containing 10^5/mL fluorescent calibration beads (6 µm, CompenFlow™, Molecular Probes, PoortGebouw, The Netherlands). Erythrocytes in the lavage fluid were lysed by hypoosmotic shock and the remaining cells were washed and double-stained with antibodies for monocyte markers F4/80 and CD11b (both eBioscience, Frankfurt am Main, Germany). The monocyte number related to the beads count was estimated with

help of FACScalibur flow cytometer (BD Bioscience, San Jose, CA) equipped with a 488 nm argon laser.

The assessment of vascular permeability *in situ* was performed as described by Oschatz et al. and van Teeffelen et al. [8,9]. Briefly, animals were subjected to inhalation anesthesia using isoflurane as described above and a central venous catheter was inserted into the left external jugular vein of SphK2$^{-/-}$ and WT transplanted mice. The distal ileum was partly transferred onto the prewarmed microscope slide and one image was acquired to assess the optimal exposure time for the exclusion of background signal. Subsequently, DyL-LDL (500 µg/animal) diluted in PBS was injected *i.v*. To provide a chemotactic stimulus, the exposed tissue was treated with bradykinin (1.0 µg/mL, Sigma, Deisenhofen, Germany) and individual micrographs were taken at two-minute intervals within a total period of 15 min. The evaluation of the DyL-LDL distribution inside and outside the blood vessels before and after bradykinin treatment as well as the quantification of protein clusters were performed off-line using ImageJ and AxioVision microscope (Carl Zeiss, Jena, Germany).

Leukocyte differential count and lymphocyte subtyping – Differential leukocyte count was performed manually (Pappenheim staining) in a routine hospital laboratory. Lymphocyte subtyping was performed by flow cytometry. Briefly, whole blood was anti-coagulated with citrate, incubated for 30 minutes with FITC- or phycoerythrin (PE)-conjugated antibodies against CD3, CD4 or CD8 (5.0 µg/mL, eBioscience), and fixed for 30 minutes with 0.4 % formaldehyde in phosphate buffered saline (PBS). Thereafter, cells were centrifuged for 10 minutes at 1700 rpm and erythrocytes were lysed in a buffer containing 0.15 mol/L NH_4Cl, 10 mmol/L $NaHCO_3$, 0.1 mmol/L EDTA (pH 7.4). The remaining cells were washed twice in PBS and analyzed on a FACSCalibur flow cytometer.

Tissue harvesting and cell immunophenotyping - Spleens were excised and single-cell suspensions were prepared by passing crude cell suspensions through a 70 µm mesh filter. Erythrocytes in cell suspensions were lysed by hypo-osmotic shock as described above. Peritoneal leukocytes were isolated by peritoneal lavage (ice-cold PBS) as described previously [2,7]. Cells were suspended in Dulbecco-modified Eagle' medium (DMEM) containing fetal calf serum (FCS, PAA Laboratories, Cölbe, Germany, 10.0 % v/v) and 2 mmol/L glutamine and were either used for flow cytometry or seeded in a 24-well plate at a density of 0.5 x 10^6 cells/mL. After 4 h non-adherent cells were removed, and remaining macrophages were incubated for 24 h in the absence or presence of LPS. Peritoneal leukocytes were immunophenotyped by flow cytometry (FACSCalibur). Monoclonal antibodies for flow cytometry were from BD Bioscience (CD86) or eBioscience (F4/80 and MHCII). For each FACS staining 2x10^5 cells were incubated with antibody dilutions (0.25 µg for each antibody) in PBS plus 1.0 % (v/v) FCS at 4ºC.

Determination of cytokine, chemokine and adhesion molecule levels – Concentrations of cytokines (TNFα, IFNγ, IL-2, IL-12), chemokines (MCP-1, RANTES) and soluble adhesion molecules (sVCAM1, sICAM1) were quantified in plasma and/or supernatants of peritoneal leukocytes and splenocytes by commercially available ELISAs (R&D Systems, Wiesbaden, Germany).

Endothelial adhesion and permeability assays – Murine endothelial cell line bEnd.5 was a generous gift of Dr. Sigrid März, Max-Planck-Institute for Molecular Medicine, Münster, and was maintained in DMEM supplemented with glutamine (2.0 %, v/v), sodium pyruvate (1.0 %, v/v), non-essential amino acids (1.0%, v/v), FCS (20.0 %, v/v), and endothelial cell growth supplement (Promocell, Heidelberg, Germany) containing epidermal growth factor (EGF) and basic fibroblast growth factor (bFGF). Humane monocyte line U937 was obtained from LGC Standards (Wesel, Germany),

and was maintained in DMEM with FCS (10.0 %, v/v). S1P (1.0 µmol/L or 2.0 µmol/L in some experiments) was added directly to cell culture media. For the assessment of monocyte adhesion, U937 cells were labeled for 30 min at 37°C with calcein-AM (1.0 µmol/L, Sigma) and added at a number of 4 x 10^6 cells/mL to a confluent bEnd.5 monolayer on cover slip in DMEM containing all components as described above except that 20% (v/v) FCS was replaced by 2% (v/v) FCS. The cover slip was kept for 30 min. under gentle rocking as described previously [7]. Non-adherent cells were removed thereafter by rinsing plates 3 times in PBS and the number of adherent cells was counted (>5 fields per cover slip) under fluorescence microscope Leica DM-IRE. For endothelial permeability testing, bEnd5 cells were seeded onto collagen-coated 24-well TransWell 0.4 µm or 5.0 µm pore-size culture inserts (Corning Life Sciences, Lowell, MA) at a density of 1 x 10^5 cells/well and cultured for 7 days as described above to form monolayers and exposed to S1P or murine plasma (25.0 % v/v) for 24h. After treatment, FITC-dextran (500.0 kDa) or DyL-LDL dissolved in DMEM were placed in the apical insert compartment at a final concentration of 500 µg/mL or 250 µg/mL, respectively, and allowed to equilibrate for 0.5 h. Alternatively, calcein-labeled U937 cells (4 x 10^6 cells/well) were applied apically to the insert for 4h. Samples were taken from basolateral chambers for fluorescence measurement. The results are expressed as the percentage of FITC-dextran or DyL-LDL influx or U937 migration across untreated bEnd.5 monolayers.

Analysis of gene expression by real-time quantitative RT-PCR - Total RNA was isolated from RAW264.7 cells using RNAeasy Plus Purification Kit (Qiagen, Hilden, Germany) according to manufacturer protocol. RNA was eluted in water and quantified using BioPhotometer (Eppendorf, Hamburg, Germany). The entire cDNA was synthesized from 1.0 µg of total RNA using RevertAid H Minus First Strand cDNA Synthesis Kit (Fischer Scientific, Schwerte, Germany). Fully automated RT-PCR set-

up was done on a Genesis 150 workstation (TECAN, Creilsheim, Germany) and PCR products were detected using ABI7900ht sequence detection system (Applied Biosystems, Darmstadt, Germany) in a 384-well format. PCR primer sequences were as follows: VCAM1 - forward primer: TTCGGTTGTTCTGACGTGTG, reverse primer: TACCACCCCATTGAGGGGAC. Relative gene expression was calculated by applying the $2^{-\Delta\Delta Ct}$ method. Briefly, the threshold cycle number (Ct) of target genes was subtracted from the Ct of GAPDH ($Ct_{housekeeping}$) and raised to the 2^{nd} power of this difference.

General Procedures - Data are presented as means ± S.D. for at least three separate experiments or as results representative for at least three repetitions. Comparisons between the means of two or multiple groups were performed with two-tailed Student t-test or one-way ANOVA for independent samples, respectively. Pairwise comparisons were performed thereafter with Student-Newman-Keuls post-hoc test. *p* values less than 0.05 were considered significant.

SUPPLEMENTARY FIGURES

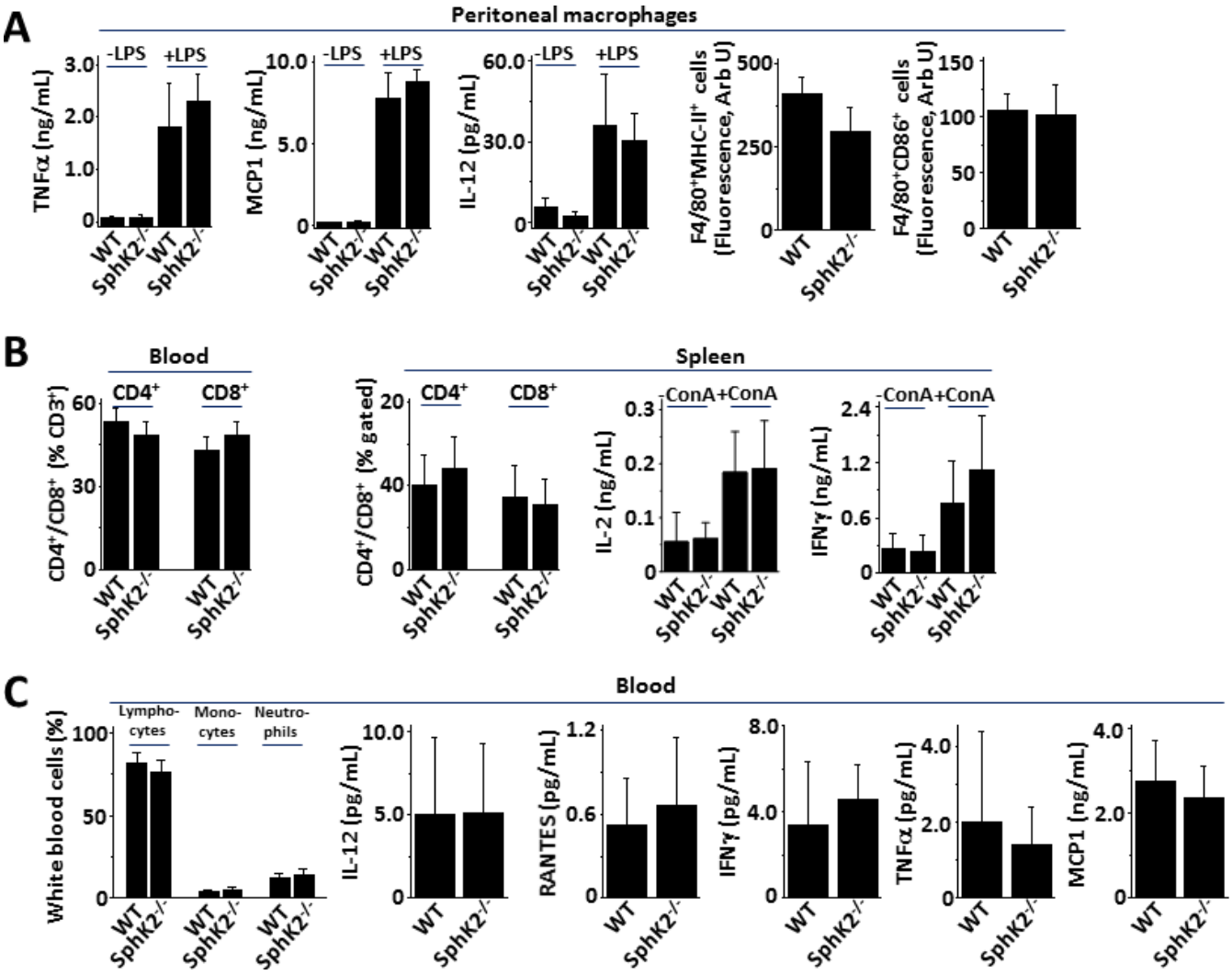

Figure I*. Hematopoietic SphK2 deficiency does not affect macrophage function* - LDL-R$^{-/-}$ mice transplanted with SphK2$^{-/-}$ (n=11) or WT (n=11) BM were placed on a Western-type diet for 14 weeks and sacrificed by exsanguination. Peritoneal cells and splenocytes were isolated as described under Material and Methods. **A**. Adherent peritoneal cells were established in culture, incubated for 24 h in the absence or presence of LPS (20.0 ng/mL) and TNFα, MCP-1 and IL-12 concentrations in medium were determined using ELISA. Single peritoneal cell suspensions were stained with antibodies against F4/80, CD86, and MHCII and analyzed by flow cytometry. Data are presented as fluorescence intensity. **B.** Blood or single cell suspensions from spleen were stained with antibodies against CD3, CD4 or CD8 and analyzed by flow cytometry. Data are presented as relative cell numbers. Splenocytes were seeded in 96 well plates and left untreated or stimulated with ConA (10.0 µg/mL) for 96 h. IFNγ and IL-2 concentrations in supernatants were determined by ELISA. **C.** Differential blood was assessed using routine laboratory method. Cytokine and chemokine concentrations in plasma were determined with ELISA.

REFERENCES TO SUPPLEMENTAL MATERIAL

1. Mizugishi K, Yamashita T, Olivera A, et al. Essential role for sphingosine kinases in neural and vascular development. Mol Cell Biol 2005;25:11113-21
2. Nofer JR, Bot M, Brodde M, et al. FTY720, a synthetic sphingosine 1 phosphate analogue, inhibits development of atherosclerosis in low-density lipoprotein receptor–deficient mice. Circulation. 2007;115:501–8.
3. Ceglarek U, Dittrich J, Helmschrodt C, et al. Preanalytical standardization of sphingosine-1-phosphate, sphinganine-1-phosphate and sphingosine analysis in human plasma by liquid chromatography-tandem mass spectrometry. Clin Chim Acta. 2014;435:1-6
4. Eschert H, Sindermann JR, Scheld HH, et al. Vascular remodeling in ApoE-deficient mice: diet dependent modulation after carotid ligation. Atherosclerosis. 2009;204:96-104
5. Nitschke Y, Weissen-Plenz G, Terkeltaub R, et al. Npp1 promotes atherosclerosis in ApoE knockout mice. J Cell Mol Med. 2011;15:2273-83
6. Potì F, Gualtieri F, Sacchi S, et al. KRP-203, sphingosine 1-phosphate receptor type 1 agonist, ameliorates atherosclerosis in LDL-R−/− mice. Arterioscler Thromb Vasc Biol. 2013;33:1505–12.
7. Poti F, Bot M, Costa S, et al. Sphingosine kinase inhibition exerts both pro- and anti-atherogenic effects in low-density lipoprotein receptor-deficient (LDL-R(-/-)) mice. Thromb Haemost. 2012;107:552-61.
8. Oschatz C, Maas C, Lecher B, et al. Mast cells increase vascular permeability by heparin-initiated bradykinin formation in vivo. Immunity. 2011;34:258-68.
9. VanTeeffelen JW, Constantinescu AA, Brands J, et al. Bradykinin- and sodium nitroprusside-induced increases in capillary tube haematocrit in mouse cremaster

muscle are associated with impaired glycocalyx barrier properties. J Physiol. 2008;586:3207-18.